

Comparison Tests of Variable-Stepsize Algorithms for Stochastic Ordinary Differential Equations of Finance

Yin Mei Wong¹ and Joshua Wilkie²

¹ Innovative Stochastic Algorithms, Vancouver,
British Columbia V6E 2C8, Canada

² Department of Chemistry, Simon Fraser University,
Burnaby, British Columbia V5A 1S6, Canada

(Dated: January 30, 2022)

Abstract

Since the introduction of the Black-Scholes model stochastic processes have played an increasingly important role in mathematical finance. In many cases prices, volatility and other quantities can be modeled using stochastic ordinary differential equations. Available methods for solving such equations have until recently been markedly inferior to analogous methods for deterministic ordinary differential equations. Recently, a number of methods which employ variable stepsizes to control local error have been developed which appear to offer greatly improved speed and accuracy. Here we conduct a comparative study of the performance of these algorithms for problems taken from the mathematical finance literature.

I. INTRODUCTION

Stochastic processes play an increasingly important role in mathematical finance as evidenced by the large and growing literature on stochastic volatility models [1, 2, 3, 4, 5, 6, 7, 8, 9, 10, 11, 12]. Often these theories are expressed in terms of stochastic ordinary differential equations (SODEs). Examples include the Cox-Ingersoll-Ross [1, 2, 3], Hull-White [4, 5, 6], Log Ornstein-Uhlenbeck [7], Nelson [8], Andersen [11] and Log-linear [12] models of stochastic volatility. Other schemes like ARCH models [8, 13] use discrete time difference equations which can be viewed as approximations to diffusions [8], and which are often favored for computational and other reasons. SODE based models tend to have closer relationships to fundamental theory, but have the drawback that analytic solutions are rarely known. In general these equations must be solved using numerical approximation schemes.

Numerical methods for SODEs have a long history [14] but until recently these algorithms have not achieved the speed and accuracy characteristic of analogous methods for deterministic ordinary differential equations (ODEs) [15]. This is partly due to the lack of variable-stepsize algorithms which allow for the control of local error, and partly due to a lack of sufficiently high order algorithms. The MAPLE Stochastic Package [16], for example, fails to include variable-stepsize routines and most methods are of rather low order. Potential solutions to both of these problems have been reported in the last few years. Discussions of variable stepsize strategies for SODEs [17, 18] and some basic observations regarding Taylor expansions for SODEs [19] have led to the emergence of a number of published [20] and unpublished [21] variable-stepsize codes. These algorithms also have a number of promising additional features such as linear scaling of computational cost with numbers of Wiener processes.

In this manuscript we perform a variety of tests to see whether the algorithms give the expected improved performance and accuracy. We refer to the method developed by Wilkie and Cetinbas [19, 20] as SDE9, and the unpublished commercial method [21] as ANISE. We will not attempt to discuss how these codes work but merely focus on their performance. We do not consider other variable-stepsize codes such as the weak method introduced in Ref. [20] since they have restricted domains of applicability.

The methods SDE9 and ANISE when applied to an Itô stochastic differential equation

$$dX_t = a(X_t; t)dt + \sum_{i=1}^n b_i(X_t; t)dW_{it} \quad (1)$$

for an observable X_t with Wiener processes W_{it} require knowledge of the partial derivatives of the solutions, i.e.,

$$\frac{\partial X_t}{\partial W_{it}} = b_i(X_t; t) \quad (2)$$

$$\frac{\partial X_t}{\partial t} = a(X_t; t) - \frac{1}{2} \sum_{i=1}^n \frac{\partial b_i(X_t; t)}{\partial W_{it}} : \quad (3)$$

All of the problems we consider are formulated with Itô stochastic differential equations and we provide these derivatives for each problem. ANISE and SDE9 are more easily applied to Stratonovich stochastic differential equations

$$dX_t = a(X_t; t)dt + \sum_{i=1}^n b_i(X_t; t) dW_{it} \quad (4)$$

for which

$$\frac{\partial X_t}{\partial W_{it}} = b_i(X_t; t) \quad (5)$$

$$\frac{\partial X_t}{\partial t} = a(X_t; t) : \quad (6)$$

Extensions to jump diffusions[12] are also straightforward, but are not considered here.

Our study shows that both SDE9 and ANISE yield accurate solutions to a wide variety of stochastic volatility models. ANISE tends to be about twice as fast as SDE9. For one problem we find that ANISE performs hundreds of times faster than SDE9. Both methods provide a means of obtaining high accuracy solutions to SODE problems, and may prove to be useful quantitative tools for further research in mathematical finance.

In section II we explore Monte-Carlo convergence of numerically calculated means and variances of price and volatilities for seven stochastic volatility models taken from the finance literature. Section III examines the accuracies of the algorithms for individual trajectories.

II. MONTE-CARLO CONVERGENCE TESTS

Here our goal is to test the accuracy and compare computational performance for the ANISE and SDE9 numerical methods for SODEs discussed in the introduction. To do this

we compare exact and numerically calculated average quantities like mean price and mean volatility for a selection of models from the finance literature.

For each model we compare known exact average quantities $\overline{X_t}$ to the numerical averages $\overline{X_{\text{approx}}} = \frac{1}{N} \sum_{j=1}^N X_t^{(j)}$ computed from individual stochastic evolutions $X_t^{(j)}$ for $j = 1; \dots; N$, obtained using the SODE methods. We examine convergence to the exact solution by varying the number of trajectories N . For each observable $\overline{X_t}$ we calculate the base ten log of the mean relative error,

$$\log_{10} \left[\frac{\overline{X_t} - \overline{X_{\text{approx}}}}{\max_j \overline{X_t} - \min_j \overline{X_{\text{approx}}}} \right]; \quad (7)$$

and plot this against time. This specific denominator, $\max_j \overline{X_t} - \min_j \overline{X_{\text{approx}}}$, is chosen since some observables X_t pass through zero and relative error can therefore blow up. We also examine the relative CPU times for the two methods. All calculations were performed on a 600 MHz Alpha processor with a requested tolerance of 10^{-12} .

A. Nelson Model

In the Nelson model[8] the log-price P_t and volatility V_t obey

$$\begin{aligned} dP_t &= \frac{q}{V_t} dW_{1t} \\ dV_t &= (-\frac{1}{2} V_t) dt + \frac{p}{2} V_t dW_{2t}; \end{aligned}$$

where the normally distributed real stochastic differentials are uncorrelated and have $\overline{dW_{it}} = 0$ and $\overline{dW_{it}^2} = dt$. Thus, this model has two Wiener processes and two equations.

The derivatives required by the SODE methods are given in Table I. We employed a time step $dt = .1$ and integrated to 100. As with ODE methods, the intermediate steps taken in

X_t	$\frac{\partial X_t}{\partial t}$	$\frac{\partial X_t}{\partial W_{1t}}$	$\frac{\partial X_t}{\partial W_{2t}}$
P_t	0	$\frac{q}{V_t}$	0
V_t	$(-\frac{1}{2} V_t)$	V_t	$\frac{p}{2} V_t$

TABLE I: Derivatives for Nelson Model.

ANISE and SDE9 do not necessarily reflect certain aspects of the true solutions such as the positivity of V_t . To avoid floating point problems one thus programs $\frac{q}{|V_t|}$ rather than $\frac{q}{V_t}$.

The actual solutions returned for V_t will of course satisfy positivity as we will see in section III where we explore the accuracy of individual trajectories.

We explored convergence for the average quantities $\overline{P_t}$, $\text{var}(P_t)$, $\overline{V_t}$, and $\text{var}(V_t)$. The known exact solutions for these quantities are given by

$$\overline{P_t} = P_0 \quad (8)$$

$$\text{var}(P_t) = \sigma^2 t + \frac{\sigma^2 V_0}{1} (e^{-\sigma^2 t} - 1) \quad (9)$$

$$\overline{V_t} = V_0 e^{-\sigma^2 t} + \frac{\sigma^2}{1} (1 - e^{-\sigma^2 t}) \quad (10)$$

$$\begin{aligned} \text{var}(V_t) = & V_0^2 e^{-2\sigma^2 t} + \frac{\sigma^4}{1} (1 - e^{-2\sigma^2 t}) \\ & - \frac{2\sigma^2 (1 - V_0)}{1} (e^{-\sigma^2 t} - e^{-2\sigma^2 t}) - \overline{V_t}^2 : \end{aligned} \quad (11)$$

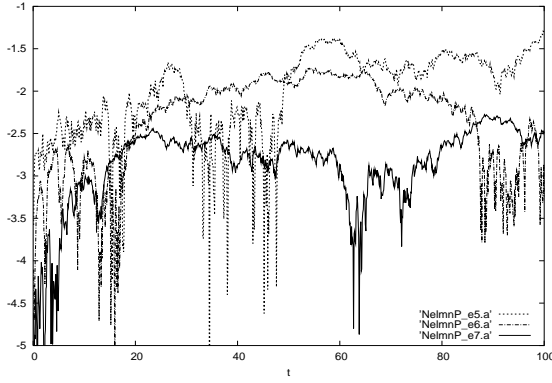
We chose parameters $\sigma = .035$, $\sigma^2 = .001225$, $V_0 = .296$, and set initial price and volatility to $P_0 = .5$ and $V_0 = .029$.

In Fig. 1 we plot the log base ten mean relative error in mean price $\overline{P_t}$ against time for ANISE (in part (a)) and SDE9 (in part (b)). Results are shown for 10^5 (dashed curve), 10^6 (dot-dashed curve) and 10^7 (solid curve) trajectories. Convergence with increasing numbers of trajectories is good in both cases. For ten million trajectories the averages have a relative accuracy of about one part in a thousand. Errors this small are not visible in plots and so we do not show the actual solutions. The requirement of millions to tens of millions of trajectories for full convergence is typical of systems of SODEs with white noises, since Monte Carlo error bounds scale as the inverse square root of the number of trajectories.

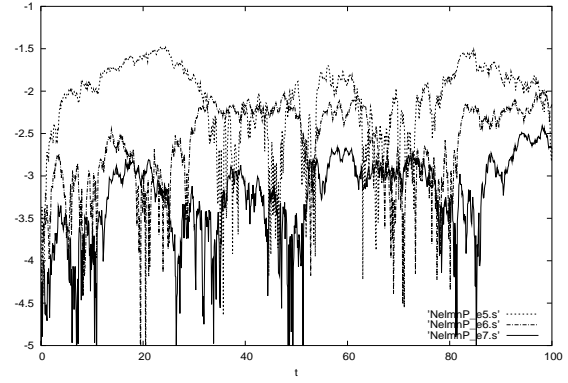
Figure 1 also shows plots of the log base ten mean relative error in variance of price $\text{var}(P_t)$ against time for ANISE (in part (c)) and SDE9 (in part (d)). Here the convergence is slightly better than that for mean price.

In Fig. 2 we show plots of the log base ten mean relative errors in the mean and variance of the volatility V_t . Here the variance has larger error than the mean. Again ANISE and SDE9 show similar rates of convergence.

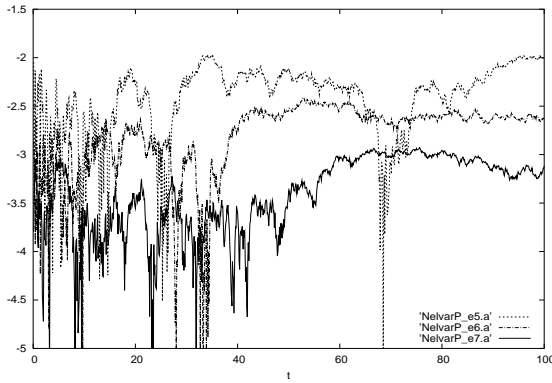
The CPU times for various numbers of trajectories are shown in Table II. ANISE takes about 7 seconds to compute 1000 trajectories. The SDE9 calculations take about 60% longer. This table also shows that both methods scale well with the number of trajectories. In other words there are no rare problematic trajectories.



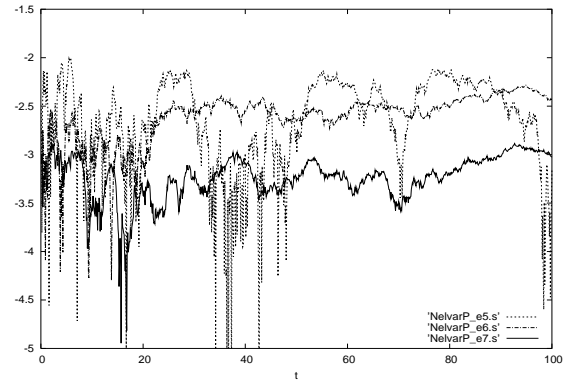
(a) Error in \overline{P}_t vs. t for ANISE .



(b) Error in \overline{P}_t vs. t for SDE9 .



(c) Error in $\text{var}(P_t)$ vs. t for ANISE .



(d) Error in $\text{var}(P_t)$ vs. t for SDE9 .

FIG .1: Error in mean and variance of P_t for Nelson model.

B . Hull-W hite M odel

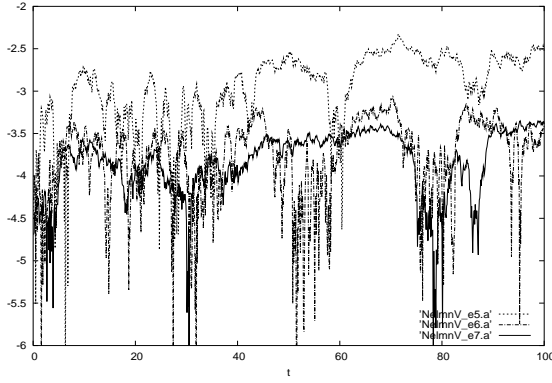
For the Hull-W hite m odel[4, 5, 6] the log-price P_t and volatility V_t obey SODEs

$$\begin{aligned} dP_t &= \frac{q}{V_t} dW_{1t} \\ dV_t &= (\quad V_t)dt + \quad dW_{2t} \end{aligned}$$

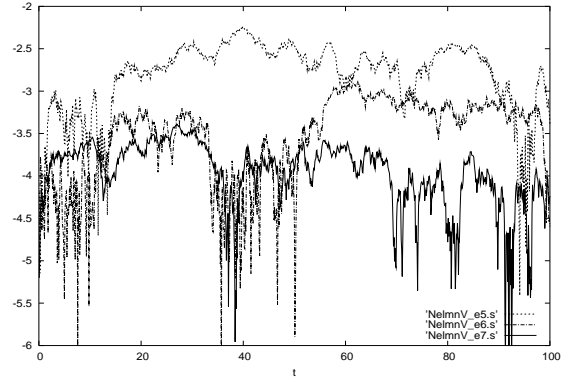
Thus, we again have two equations and two Wiener processes.

The derivatives needed by the numerical methods are given in Table III. A time step of $dt = :1$ was used and the equations were integrated to 100. Once again care must be taken to program $\frac{q}{V_t}$ rather than $\frac{P}{V_t}$.

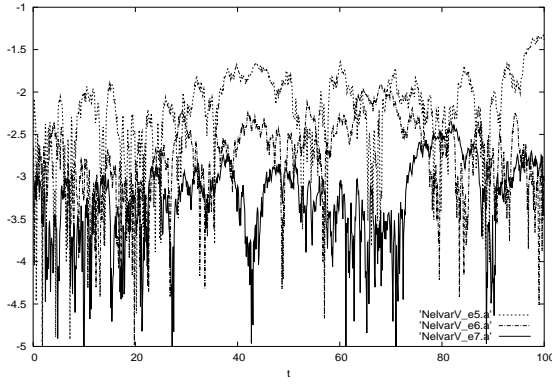
We explored convergence for the average quantities \overline{P}_t , $\text{var}(P_t)$, \overline{V}_t , and $\text{var}(V_t)$. The



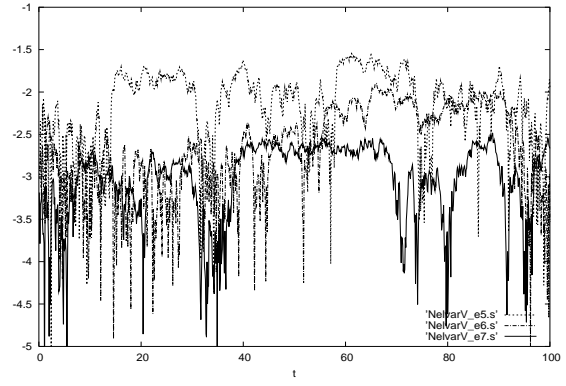
(a) Error in \overline{V}_t vs. t for ANISE .



(b) Error in \overline{V}_t vs. t for SDE9.



(c) Error in $\text{var}(V_t)$ vs. t for ANISE .



(d) Error in $\text{var}(V_t)$ vs. t for SDE9.

FIG . 2: Error in mean and variance of V_t for Nelson model.

exact solutions for these observables are given by

$$\overline{P}_t = P_0 \quad (12)$$

$$\text{var}(P_t) = \frac{V_0}{2} (1 - e^{-t}) + \frac{1}{2} (t + e^{-t} - 1) \quad (13)$$

$$\overline{V}_t = V_0 e^{-t} + \frac{1}{2} (1 - e^{-t}) \quad (14)$$

$$\text{var}(V_t) = \frac{1}{2} (1 - e^{-2t}) \quad (15)$$

for this model.

We set parameters $\alpha = .03$, $\beta = .035$, $\gamma = .0068$, and initial conditions $V_0 = .029$ and $P_0 = .5$.

In Fig. 3 we plot the log base ten error in the mean and variance of P_t for ANISE ((a) and

# Trajectories	ANISE CPU Time	SDE9 CPU Time	CPU Time Ratio SDE9/ANISE
10^3	0.69E+ 01	0.11E+ 02	1.59
10^4	0.68E+ 02	0.11E+ 03	1.62
10^5	0.68E+ 03	0.11E+ 04	1.63
10^6	0.68E+ 04	0.11E+ 05	1.62
10^7	0.68E+ 05	0.11E+ 06	1.62

TABLE II: CPU times for Nelson Model in seconds.

X_t	$\frac{\partial X_t}{\partial t}$	$\frac{\partial X_t}{\partial W_{1t}}$	$\frac{\partial X_t}{\partial W_{2t}}$
P_t	0	$P \frac{1}{V_t}$	0
V_t	V_t	0	0

TABLE III: Derivatives for Hull-White Model.

(c), respectively) and for SDE9 ((b) and (d), respectively). Dotted curves show the results for 10^5 trajectories while dot-dashed and solid curves are for 10^6 and 10^7 trajectories, respectively. Good convergence with numbers of trajectories is seen. Once again, convergence for the variance is slightly better than that for the mean.

Figure 4 shows the log base ten error in the mean and variance of the volatility V_t for ANISE ((a) and (c), respectively) and for SDE9 ((b) and (d), respectively). Again good convergence to the exact results is observed. The errors in the variance are larger than those in the mean.

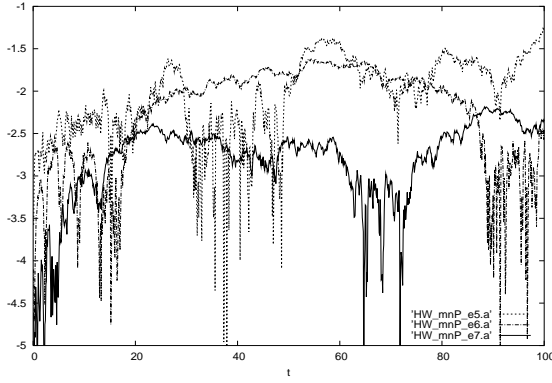
Cpu times are compared in Table IV for various numbers of trajectories. ANISE takes 7.5 s to compute 1000 trajectories. Again we observe that SDE9 takes 50 % longer. Once again good scaling is obtained for both methods with the number of trajectories.

C. Cox-Ingersoll-Ross Model

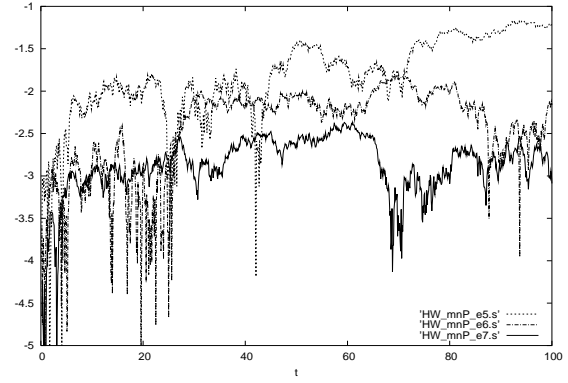
The SODEs for the Cox-Ingersoll-Ross model [2] are

$$dP_t = \left(\frac{q}{dt} + \frac{1}{V_t} dW_{1t} \right) P_t \quad (16)$$

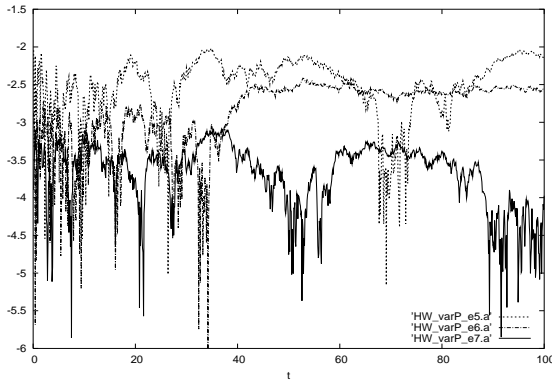
$$dV_t = \left(\frac{q}{V_t} dt + \frac{1}{V_t} [dW_{1t} + \frac{1}{2} dW_{2t}] \right) V_t \quad (17)$$



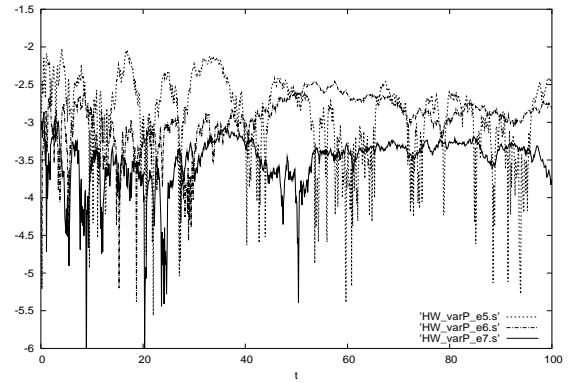
(a) Error in $\overline{P_t}$ vs. t for ANISE .



(b) Error in $\overline{P_t}$ vs. t for SDE9 .



(c) Error in $\text{var}(P_t)$ vs. t for ANISE .



(d) Error in $\text{var}(P_t)$ vs. t for SDE9 .

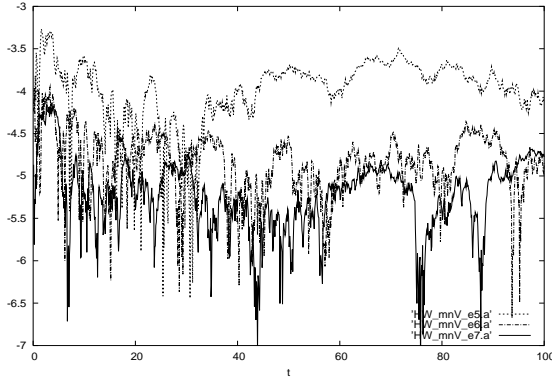
FIG . 3: Error in mean and variance of P_t for Hull-White model.

and so we have two equations with two Wiener processes. In this case the volatility depends on both Wiener processes.

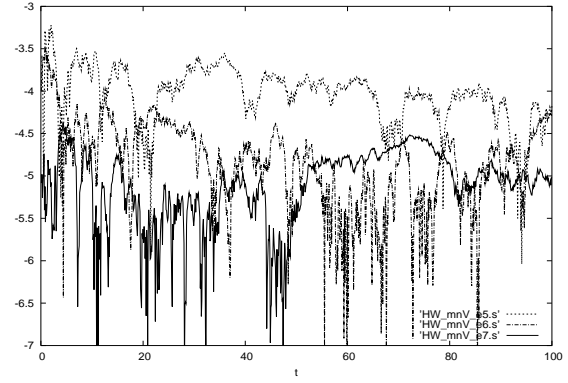
The derivatives needed by the numerical methods are provided in Table V. A time step of $dt = .01$ was used and the equations were integrated to 10.

We look for convergence in four observables; mean log-price $\overline{\ln P_t}$, variance in log-price $\text{var}(\ln P_t)$, mean volatility $\overline{V_t}$, and variance of the volatility $\text{var}(V_t)$. The exact solutions for these quantities are given by

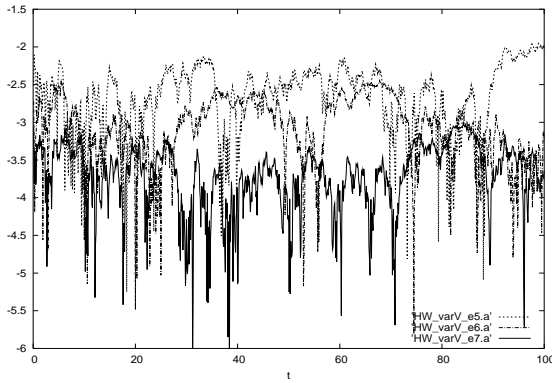
$$\begin{aligned} \overline{\ln P_t} &= \ln P_0 + \left(-\frac{\gamma}{2} \right) t + \frac{1}{2} (V_0 - \gamma) (e^{-\gamma t} - 1) \\ \text{var}(\ln P_t) &= \left[\frac{\gamma^2}{4} - \left(\frac{\gamma}{4} \right) \right] t + - (V_0 - \gamma) \left(\frac{\gamma}{2} \right) t e^{-\gamma t} \end{aligned} \quad (18)$$



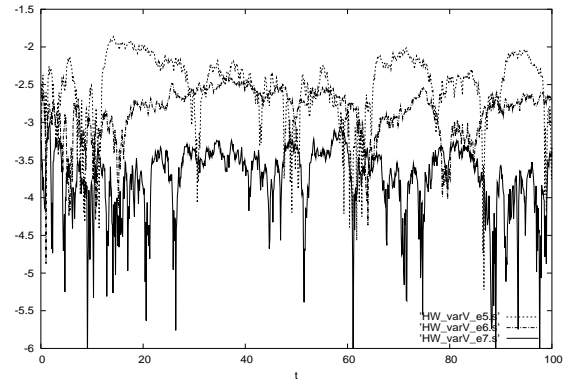
(a) Error in \overline{V}_t vs. t for ANISE .



(b) Error in \overline{V}_t vs. t for SDE9 .



(c) Error in $\text{var}(V_t)$ vs. t for ANISE .



(d) Error in $\text{var}(V_t)$ vs. t for SDE9 .

FIG . 4: Error in mean and variance of V_t for Hull-White model.

$$+ \frac{f}{2} \left[(V_0 - \frac{V_0}{2}) \left(\frac{1}{2} - \left(\frac{1}{4} \right) \right) \right] \frac{V_0}{2} g(e^{-t} - 1) \\ + \frac{f^2}{4^3} (V_0 - \frac{V_0}{2}) (e^{-t} - 1)^2 \quad (19)$$

$$\overline{V}_t = V_0 e^{-t} + \frac{1}{2} (1 - e^{-t}) \quad (20)$$

$$\text{var}(V_t) = \frac{V_0^2}{2} (e^{-t} - e^{-2t}) + \frac{f^2}{2} (1 - e^{-t})^2 \quad (21)$$

The parameters were set to $\alpha = .1$, $\beta = .29368$, $\gamma = .07935$, $\delta = .11425$, $\sigma = .2$ and price and volatility was set to initial values $P_0 = 1$ and $V_0 = .1$.

In Fig. 5 we show the log base ten error in $\ln P_t$ and $\text{var}(\ln P_t)$ plotted against time for ANISE ((a) and (c)) and SDE9 ((b) and (d)). Dashed, dot-dashed and solid curves represent errors for runs of 10^5 , 10^6 and 10^7 trajectories, respectively. Good convergence is seen for

# Trajectories	ANISE CPU Time	SDE9 CPU Time	CPU Time Ratio SDE9/ANISE
10^3	0.76E+ 01	0.11E+ 02	1.47
10^4	0.76E+ 02	0.11E+ 03	1.44
10^5	0.76E+ 03	0.11E+ 04	1.46
10^6	0.76E+ 04	0.11E+ 05	1.46
10^7	0.76E+ 05	0.11E+ 06	1.46

TABLE IV : CPU times for Hull-White in seconds.

X_t	$\frac{\partial X_t}{\partial t}$	$\frac{\partial X_t}{\partial W_{1t}}$	$\frac{\partial X_t}{\partial W_{2t}}$
P_t	$(\frac{1}{2}(V_t + \frac{1}{2}))P_t$	$P_t^P \overline{V}_t$	0
V_t	$(V_t) \frac{1}{4}^2$	$P \overline{V}_t$	$P \frac{1}{1}^2 P \overline{V}_t$

TABLE V : Derivatives for Cox-Ingersoll-Ross Model.

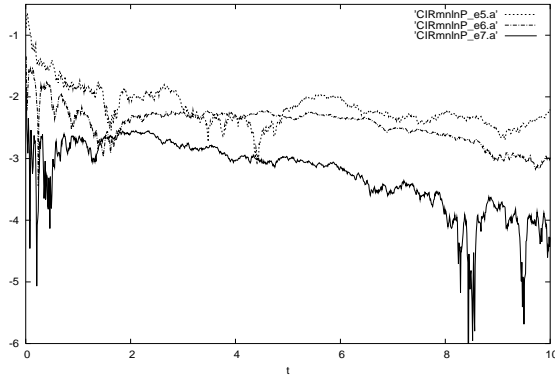
both methods at all times, although errors in the variance are larger than those in the mean.

Figure 6 plots errors in \overline{V}_t and $\text{var}(V_t)$. Again we see excellent convergence in both cases. Errors in the variance are bigger than those in the mean.

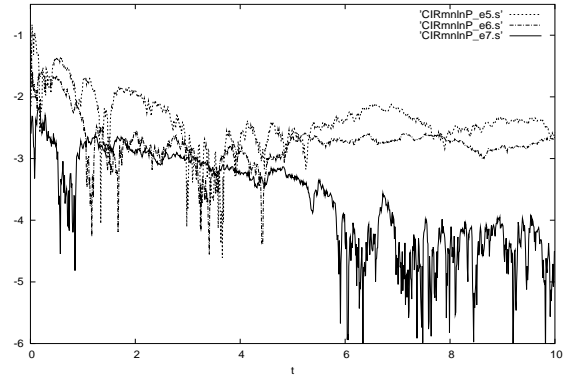
The cpu times for various numbers of trajectories are shown in Table VI. ANISE takes less than 5 s to compute 1000 trajectories. The ratio of cpu time for SDE9 to that of ANISE is now a much larger 2.5. This relative slowing down of SDE9 is probably caused by the fact that V_t now depends on two Wiener processes. Once again the ratio is independent of the number of trajectories indicating that both methods handle all trajectories equally well.

# Trajectories	ANISE CPU Time	SDE9 CPU Time	CPU Time Ratio SDE9/ANISE
10^3	0.48E+ 01	0.12E+ 02	2.45
10^4	0.48E+ 02	0.12E+ 03	2.46
10^5	0.48E+ 03	0.12E+ 04	2.46
10^6	0.48E+ 04	0.12E+ 05	2.47
10^7	0.48E+ 05	0.12E+ 06	2.47

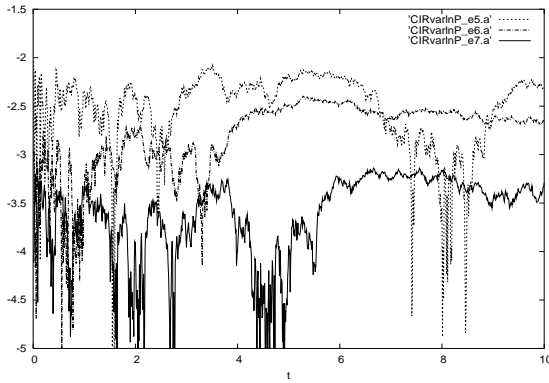
TABLE VI: CPU times for Cox-Ingersoll-Ross model in seconds.



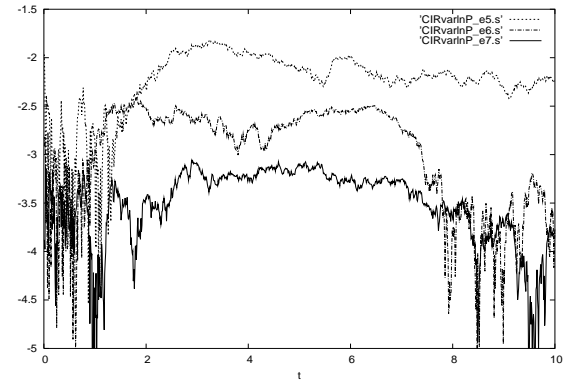
(a) Error in $\overline{\ln P_t}$ vs. t for ANISE .



(b) Error in $\overline{\ln P_t}$ vs. t for SDE9 .



(c) Error in $\text{var}(\ln P_t)$ vs. t for ANISE .



(d) Error in $\text{var}(\ln P_t)$ vs. t for SDE9 .

FIG . 5: Error in mean and variance of $\ln P_t$ for Cox-Ingersoll-Ross model.

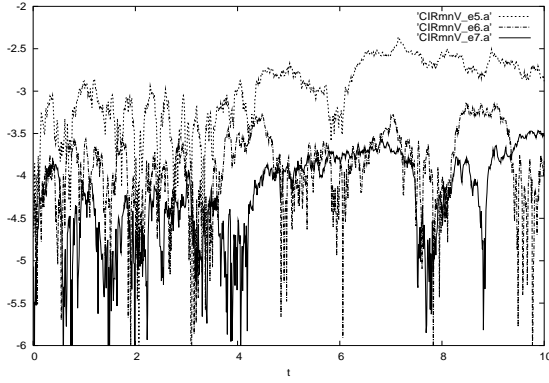
D . Log-O mstein-U hlenbeck M odel

The fourth example is the Log O mstein-U hlenbeck model[7] for price P_t and volatility V_t . In this model

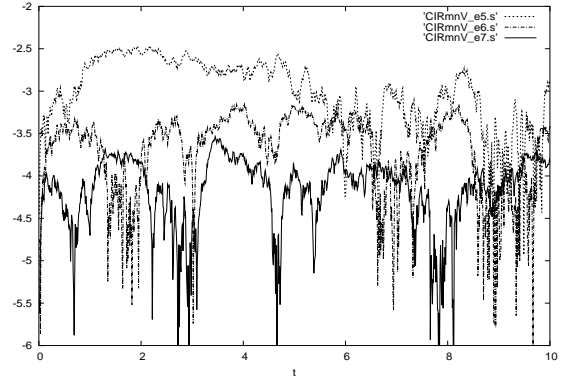
$$\begin{aligned} dP_t &= (adt + e^{V_t} dW_{1t})P_t \\ dV_t &= (a - bV_t)dt + \frac{1}{2} [dW_{1t} + \frac{q}{1} dW_{2t}]^2 \end{aligned}$$

and so we again have two equations and two Wiener processes. The volatility depends on both Wiener processes.

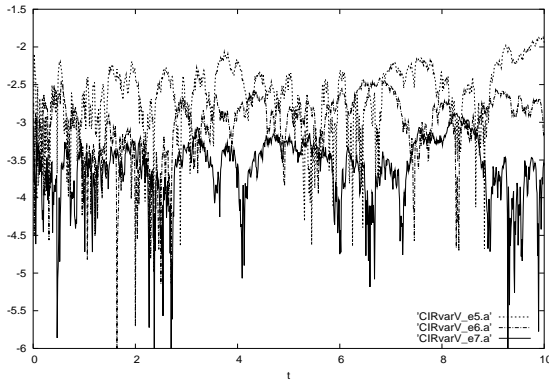
The derivatives required by the SODE methods are given in Table VII. A time step of 10^{-4} was used and the equations were integrated to 0.1.



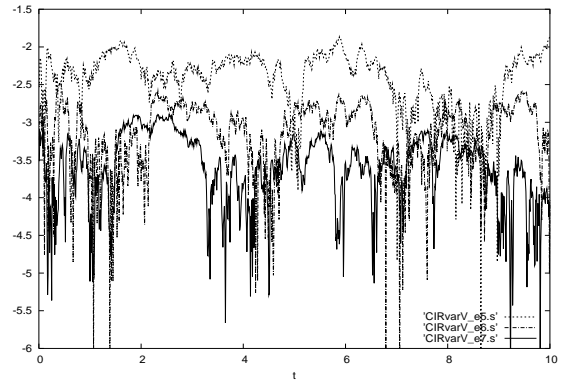
(a) Error in \overline{V}_t vs. t for ANISE .



(b) Error in \overline{V}_t vs. t for SDE9 .



(c) Error in $\text{var}(V_t)$ vs. t for ANISE .



(d) Error in $\text{var}(V_t)$ vs. t for SDE9 .

FIG . 6: Error in mean and variance of V_t for Cox-Ingersoll-Ross model.

X_t	$\frac{\partial X_t}{\partial t}$	$\frac{\partial X_t}{\partial W_{1t}}$	$\frac{\partial X_t}{\partial W_{2t}}$
P_t	$aP_t - \frac{1}{2}P_t e^{V_t} (\frac{1}{2} + e^{V_t})$	$e^{V_t}P_t$	0
V_t	$a + bV_t$	$\frac{1}{2}$	$\frac{1}{2}P \frac{1}{1 - 2}$

TABLE VII: Derivatives for Log Ornstein-Uhlenbeck Model.

We look for convergence in three quantities; mean log-price $\overline{\ln P_t}$, mean volatility $\overline{V_t}$, and variance in volatility $\text{var}(V_t)$. Exact solutions for these observables are given by

$$\overline{\ln P_t} = \ln P_0 + at - \frac{1}{2} \int_0^t dt' \exp[2V_0 e^{bt'} + \frac{a}{b}(1 - e^{bt'})] + \frac{1}{4b}(1 - e^{2bt'})g \quad (22)$$

$$\overline{V_t} = V_0 e^{bt} + \frac{a}{b}(1 - e^{bt}) \quad (23)$$

$$\text{var}(V_t) = \frac{1}{8b} (1 - e^{-2bt}) \quad (24)$$

The solution for $\overline{\ln P_t}$ was obtained using a variable-stepsize Runge-Kutta code for ODEs [15]. Parameters were set to $a = 70, b = 100, \gamma = .2$ and initial conditions $P_0 = .5$ and $V_0 = .029$ were used.

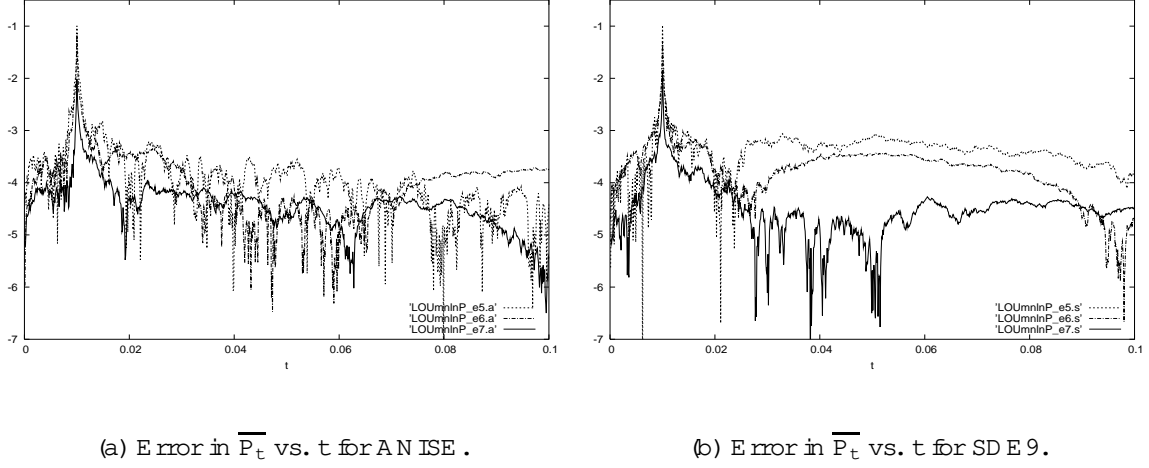
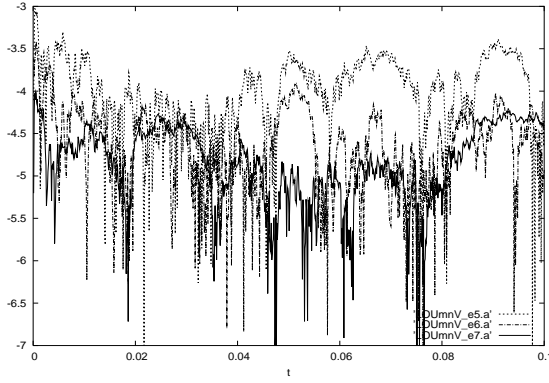


FIG. 7: Error in mean of $\ln P_t$ for Log-Oststein-Uhlenbeck model.

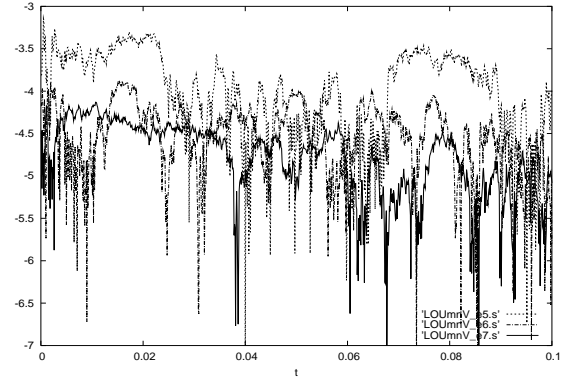
In Fig. 7 we plot the log base ten relative error in $\overline{\ln P_t}$ for ANISE in (a) and SDE9 in (b). Errors are shown for averages over 10^5 (dashed curve), 10^6 (dot-dashed curve) and 10^7 (solid curve) trajectories. In all cases a spike in error is seen near the time $t = .01$ where the exact $\overline{\ln P_t}$ passes through zero. The absolute error is small and so the spike in relative error indicated in the plots is essentially fictitious and convergence is in fact good at all times for both methods.

Figure 8 plots the mean relative error in the mean and variance of the volatility for ANISE ((a) and (c), respectively) and SDE9 ((b) and (d), respectively). The error in the variance is larger than that in the mean. Here we see good convergence for both methods at all times.

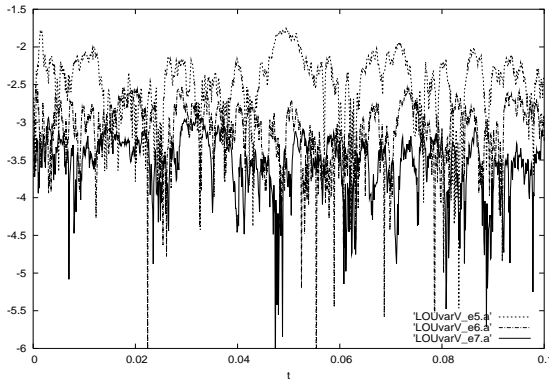
The cpu times for various numbers of trajectories are shown in Table VIII. ANISE takes about 5 s to compute 1000 trajectories. The ratio of cpu time of SDE9 to ANISE is again larger than two. The ratio is roughly independent of the number of trajectories.



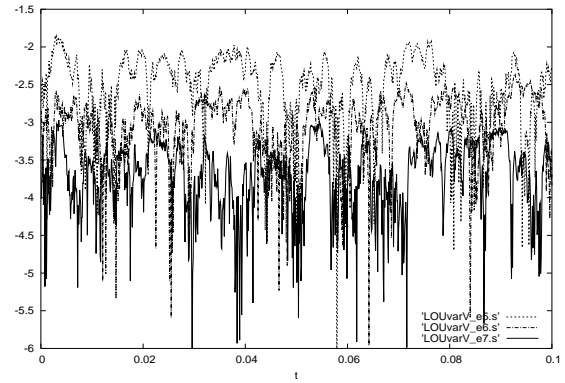
(a) Error in \overline{V}_t vs. t for ANISE .



(b) Error in \overline{V}_t vs. t for SDE 9.



(c) Error in $\text{var}(V_t)$ vs. t for ANISE .



(d) Error in $\text{var}(V_t)$ vs. t for SDE 9.

FIG . 8: Error in mean and variance of V_t for Log-O mstein-Uhlenbeck model.

E . A ne Two Volatility Factor Model

The equations for the log-price and volatilities of an a ne two volatility model[11, 12] are

$$dP_t = \frac{q}{dt} + \frac{q}{0 + 1V_{1t} + 2V_{2t}} dW_{3t} \quad (25)$$

$$dV_{1t} = (10 + 11V_{1t})dt + \frac{q}{V_{1t}} dW_{1t} \quad (26)$$

$$dV_{2t} = (20 + 21V_{2t})dt + \frac{q}{V_{2t}} dW_{2t} \quad (27)$$

and so we now have three equations and three Wiener processes.

The derivatives required by the numerical methods are given in Table IX . A time step of $dt = .001$ was employed and the equations were integrated to 0.5.

# Trajectories	ANISE CPU Time	SDE9 CPU Time	CPU Time Ratio SDE9/ANISE
10^3	0.53E+01	0.13E+02	2.46
10^4	0.52E+02	0.12E+03	2.38
10^5	0.52E+03	0.12E+04	2.29
10^6	0.52E+04	0.12E+05	2.28
10^7	0.52E+05	0.12E+06	2.29

TABLE VIII: CPU times for Log-O mstein-Uhlenbeck model in seconds.

X_t	$\frac{\partial X_t}{\partial t}$	$\frac{\partial X_t}{\partial W_{1t}}$	$\frac{\partial X_t}{\partial W_{2t}}$	$\frac{\partial X_t}{\partial W_{3t}}$
P_t		0	0	$P_0 \frac{1}{V_{1t} V_{2t}}$
V_{1t}	$10 + 11V_{1t} \frac{1}{4}$	$P_0 \frac{1}{V_{1t}}$	0	0
V_{2t}	$20 + 21V_{2t} \frac{1}{4}$	0	$P_0 \frac{1}{V_{2t}}$	0

TABLE IX : Derivatives for A ne Two Volatility Factor Model.

We exam ined quantities $\overline{P_t}$, $\text{var}(P_t)$, $\overline{V_{1t}}$, and $\text{var}(V_{1t})$ which have exact solutions given by

$$\overline{P_t} = P_0 + t \quad (28)$$

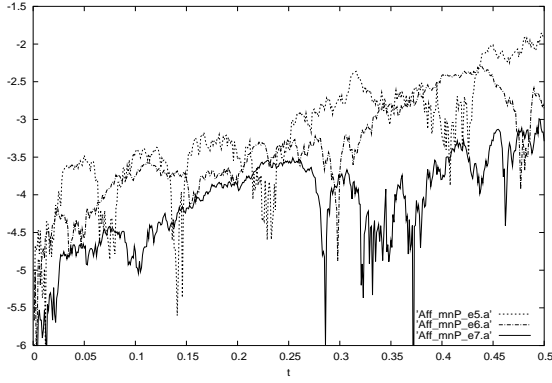
$$\begin{aligned} \text{var}(P_t) = & \left[0 \quad \frac{1}{11} \frac{10}{21} \quad \frac{2}{21} \frac{20}{11} \right] t + \frac{1}{11} \left(V_{10} + \frac{10}{11} \right) (e^{11t} - 1) \\ & + \frac{2}{21} \left(V_{20} + \frac{20}{21} \right) (e^{21t} - 1) \end{aligned} \quad (29)$$

$$\overline{V_{1t}} = V_{10} e^{11t} + \frac{10}{11} (e^{11t} - 1) \quad (30)$$

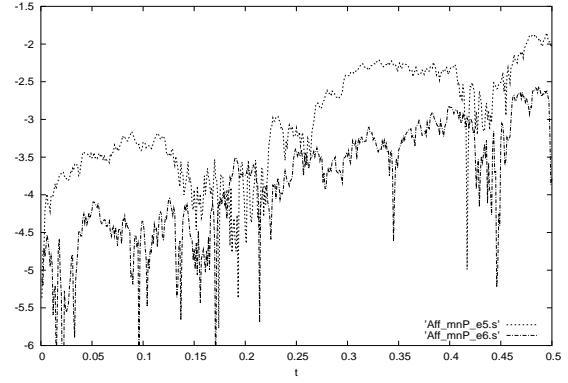
$$\text{var}(V_{1t}) = \frac{10}{2} \frac{2}{11} (e^{11t} - 1)^2 + \frac{V_{10}}{11} (e^{211t} - e^{11t}): \quad (31)$$

The param eters were set as $\sigma_0 = .01$, $\sigma_1 = .1258$, $\sigma_2 = .0344$, $\rho = .02$, $V_{10} = .2894$, $V_{11} = 17.4321$, $V_{20} = .0602$, $V_{21} = 13.6036$, $P_0 = 1$, $V_{10} = .2$, and $V_{20} = .2$. Note that on average V_{1t} increases exponentially with a large exponent, and so the noises in the equation for the price P_t are strongly weighted.

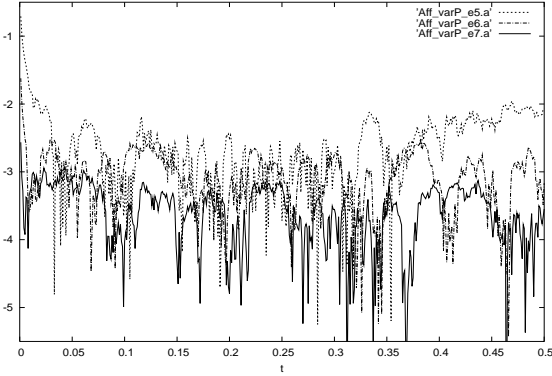
In Fig. 9 we show convergence via the log base ten relative error in the mean and variance of the price for ANISE ((a) and (c), respectively) and SDE9 (b) and (d), respectively). For ANISE the plbts show three curves corresponding to runs with averages over 10^5 (dashed



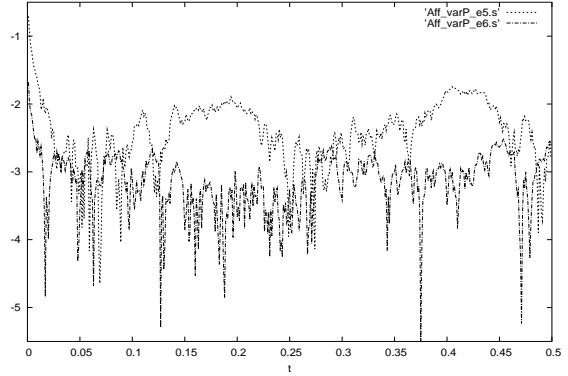
(a) Error in $\overline{P_t}$ vs. t for ANISE.



(b) Error in $\overline{P_t}$ vs. t for SDE9.



(c) Error in $\text{var}(P_t)$ vs. t for ANISE.

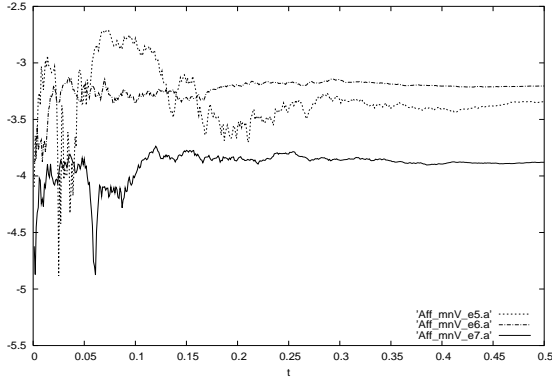


(d) Error in $\text{var}(P_t)$ vs. t for SDE9.

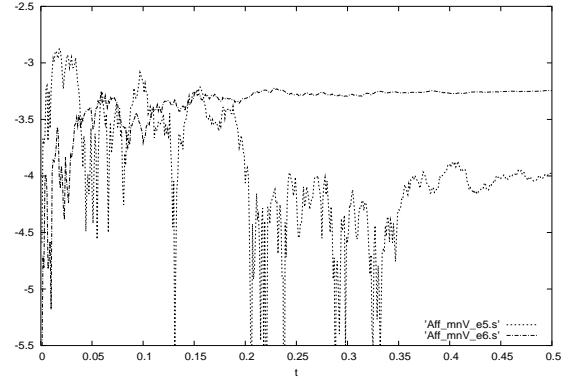
FIG. 9: Error in mean and variance of P_t for Anne model.

curve), 10^6 (dot-dashed curve), and 10^7 (solid curve) trajectories. For SDE9 the plots show just two curves corresponding to runs with averages over 10^5 (dashed curve) and 10^6 (dot-dashed curve) trajectories. In both cases good convergence is observed toward the exact solution. The error in the variance is larger than that in the mean. As we discuss below the relative cpu time for SDE9 is much larger than for previous problems. Indeed, the run with 10^7 trajectories did not finish and so does not appear in the figures.

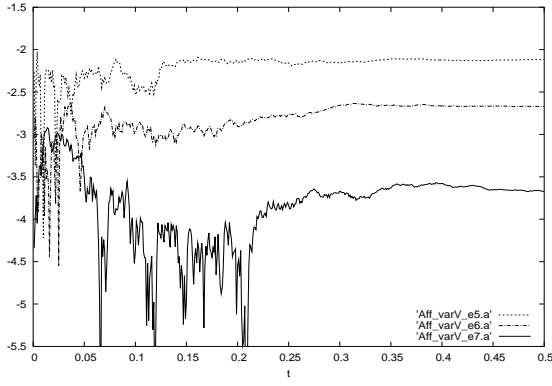
Figure 10 plots the errors in $\overline{V_{1t}}$ and $\text{var}(V_{1t})$ against time for ANISE ((a) and (c), respectively) and SDE9 (b) and (d), respectively) for the same numbers of trajectories as in the previous figure. Error in the variance is larger than that in the mean. Good convergence is again observed for both methods.



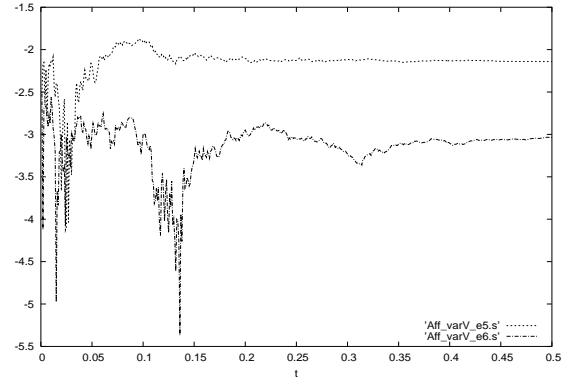
(a) Error in $\overline{V_{1t}}$ vs. t for ANISE .



(b) Error in $\overline{V_{1t}}$ vs. t for SDE9 .



(c) Error in $\text{var}(V_{1t})$ vs. t for ANISE .



(d) Error in $\text{var}(V_{1t})$ vs. t for SDE9 .

FIG .10: Error in mean and variance of V_{1t} for A ne model.

The cpu times for various numbers of trajectories are shown in Table X . ANISE takes about 3.5 s to compute 1000 trajectories. In spite of the fact that good convergence was observed for the SDE9 method its computation times show a large jump from the 10^4 calculation to the 10^5 calculation. For 10^5 and 10^6 ANISE is several hundred times faster than SDE9. Rare trajectories with difficult stochastic paths appear to be responsible for the poor performance of SDE9.

# Trajectories	ANISE CPU Time	SDE9 CPU Time	CPU Time Ratio SDE9/ANISE
10^3	0.34E+01	0.10E+02	2.96
10^4	0.34E+02	0.92E+02	2.74
10^5	0.34E+03	0.88E+05	261.61
10^6	0.34E+04	0.13E+07	386.63
10^7	0.34E+05	NA	NA

TABLE X: CPU times for A n e m o d e l in seconds.

F. Log Linear Two Volatility Factor Model Without Feedback

The price and volatilities obey [12]

$$dP_t = (r_0 + \frac{1}{2}V_{2t})dt + e^{r_0 + \frac{1}{2}V_{2t}} \left[\frac{1}{\sigma_1} dW_{1t} + \frac{1}{\sigma_3} dW_{3t} \right] P_t \quad (32)$$

$$dV_{2t} = \sigma_2^2 V_{2t} dt + \sigma_2 dW_{2t} \quad (33)$$

$$dV_{3t} = \sigma_3^2 V_{3t} dt + \sigma_3 dW_{3t} \quad (34)$$

and so we have three equations and three Wiener processes.

The derivatives needed by the numerical methods are given in Table XI. A time step of 10^{-4} was used and the equations were integrated to 0.1.

X_t	$\frac{\partial X_t}{\partial t}$	$\frac{\partial X_t}{\partial W_{1t}}$	$\frac{\partial X_t}{\partial W_{2t}}$	$\frac{\partial X_t}{\partial W_{3t}}$
P_t	$(r_0 + \frac{1}{2}V_{2t}) P_t$	$\frac{1}{\sigma_1} P_t$	0	$\frac{1}{\sigma_3} P_t$
V_{2t}	$\sigma_2^2 V_{2t}$	0	1	0
V_{3t}	$\sigma_3^2 V_{3t}$	0	0	1

TABLE XI: Derivatives for Log Linear model without feedback. Here $F_t = e^{r_0 + \frac{1}{2}V_{2t}}$.

We calculated $\overline{\ln P_t}$, $\overline{V_{2t}}$, $\overline{V_{3t}}$, and $\text{var}(V_{3t})$, some of which have known exact solutions

$$\overline{V_{2t}} = V_{20} e^{\sigma_2^2 t} \quad (35)$$

$$\overline{V_{3t}} = V_{30} e^{\sigma_3^2 t} \quad (36)$$

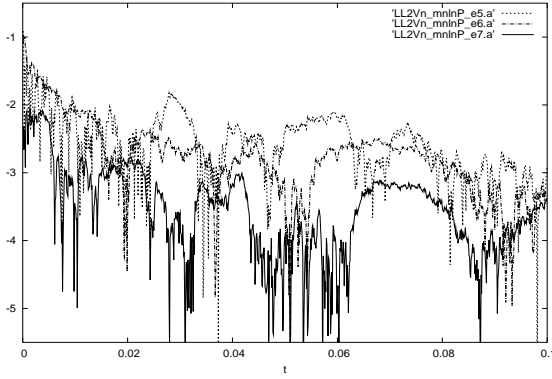
$$\text{var}(V_{3t}) = \frac{1}{2\sigma_3^2} (e^{2\sigma_3^2 t} - 1) \quad (37)$$

Once again we had to solve an ODE

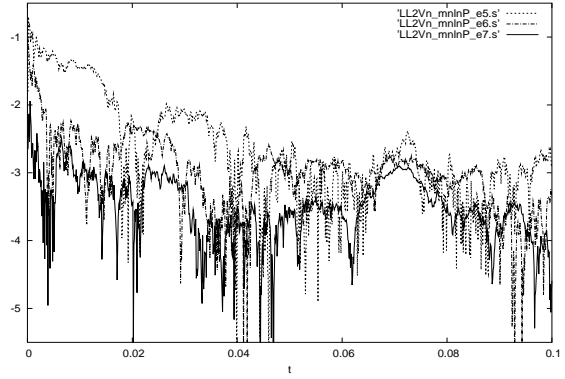
$$\frac{d\overline{\ln P_t}}{dt} = \gamma_{10} + \gamma_{12}V_{20}e^{-\gamma_{22}t} - \frac{1}{2}\exp(2\gamma_{10} + 2\gamma_{13}V_{30}e^{-\gamma_{33}t} + \frac{\gamma_{13}^2}{33}(e^{-2\gamma_{33}t} - 1))g \quad (38)$$

numerically to find $\overline{\ln P_t}$. This was again accomplished using a Runge-Kutta algorithm for ODEs[15].

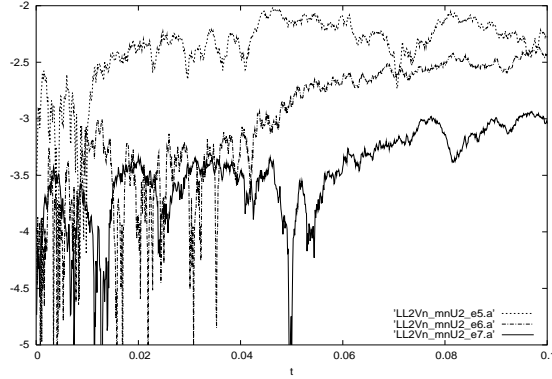
The parameters were set as $\gamma_{10} = .0337$, $\gamma_{12} = .4820$, $\gamma_{22} = 1.0043$, $\gamma_{33} = .0291$, $\gamma_{10} = 1.0294$, $\gamma_{13} = .0261$, $\gamma_{13} = .3285$, $P_0 = 1$, $V_{20} = .1$, $V_{30} = .05$.



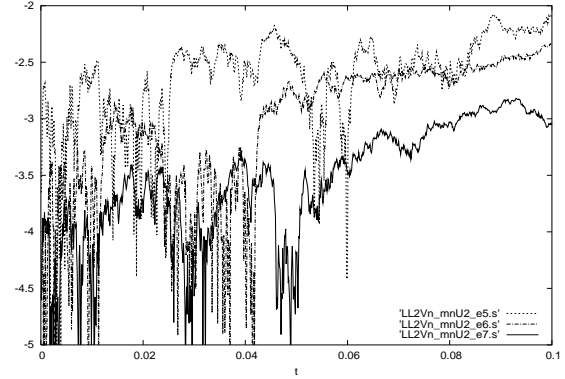
(a) $\overline{\ln P_t}$ vs. t for ANISE



(b) $\overline{\ln P_t}$ vs. t for SDE9



(c) $\overline{V_{2t}}$ vs. t for ANISE

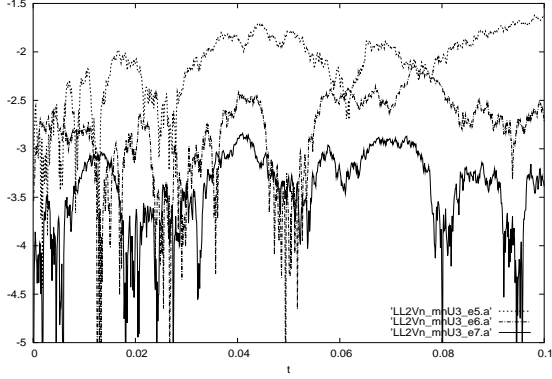


(d) $\overline{V_{2t}}$ vs. t for SDE9

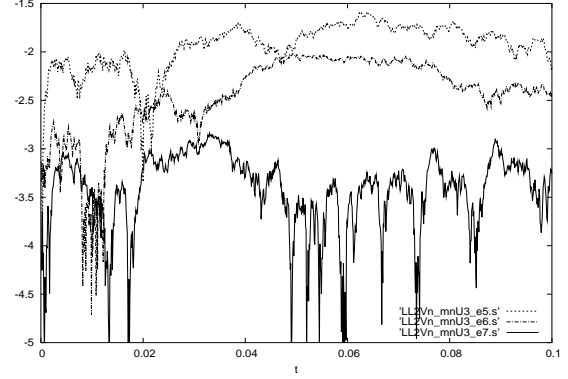
FIG .11: Means of $\ln P_t$ and V_{2t} for Log Linear model without feedback

In Fig. 11 we plot the log base ten relative error in $\overline{\ln P_t}$ and $\overline{V_{2t}}$ for ANISE ((a) and (c), respectively) and SDE9 ((b) and (d), respectively). In all cases the dashed curve represents an average over 10^5 trajectories while the dot-dashed and solid curves are for 10^6 and 10^7

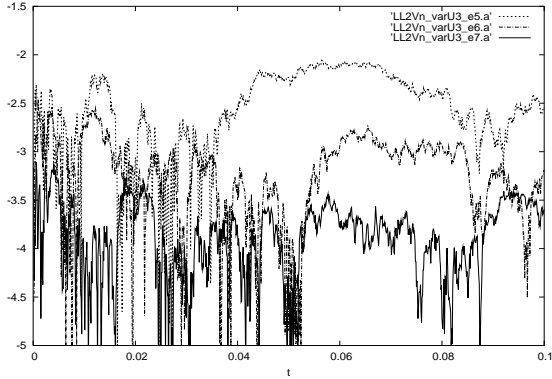
trajectories, respectively. Good convergence is seen in all cases except near $t = 0$ for $\overline{\ln P_t}$. The exact solution for $\overline{\ln P_t}$ vanishes at $t = 0$ for our initial condition, and poor relative accuracy is seen as a consequence. In fact the absolute accuracy is good at all times for 10^7 trajectories.



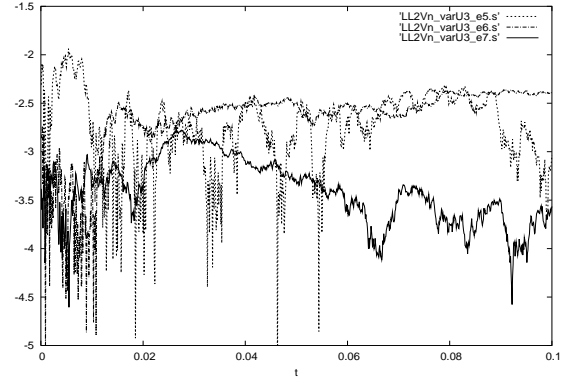
(a) $\overline{V_{3t}}$ vs. t for ANISE



(b) $\overline{V_{3t}}$ vs. t for SDE9



(c) $\text{var}(V_{3t})$ vs. t for ANISE



(d) $\text{var}(V_{3t})$ vs. t for SDE9

FIG. 12: Error in mean and variance of V_{3t} for Log Linear model without feedback

Figure 12 plots the errors in $\overline{V_{3t}}$ and $\text{var}(V_{3t})$ against time for ANISE and SDE9. Once again, good convergence is observed. Errors in the mean and variance are comparable.

The cpu times for various numbers of trajectories are shown in Table XII. ANISE takes 6.5 s to compute 1000 trajectories. Once again the ratio of cpu time for SDE9 to that of ANISE is a little greater than two and this number is independent of the number of trajectories.

# Trajectories	ANISE CPU Time	SDE9 CPU Time	CPU Time Ratio SDE9/ANISE
10 ³	0.65E+ 01	0.14E+ 02	2.11
10 ⁴	0.64E+ 02	0.14E+ 03	2.13
10 ⁵	0.64E+ 03	0.14E+ 04	2.18
10 ⁶	0.64E+ 04	0.14E+ 05	2.18
10 ⁷	0.64E+ 05	0.14E+ 06	2.17

TABLE X II: CPU times for Log Linear model without feedback in seconds.

G . Log Linear Two Volatility Factor Model With Feedback

The equations for this model [12] are

$$dP_t = f(10 + 12V_{2t})dt + e^{10 + 13V_{3t} + 14V_{4t}} \left[1 - \frac{2}{13} - \frac{2}{14} \right] dW_{1t} + 13dW_{3t} + 14dW_{4t} \log P_t \quad (39)$$

$$dV_{2t} = 22V_{2t}dt + dW_{2t} \quad (40)$$

$$dV_{3t} = 33V_{3t}dt + (1 + 33V_{3t})dW_{3t} \quad (41)$$

$$dV_{4t} = 44V_{4t}dt + (1 + 44V_{4t})dW_{4t} \quad (42)$$

In this case we have four equations and four Wiener processes.

The derivatives required by the numerical methods are given in Table X III. A time step of $dt = 10^{-4}$ was employed and the equations were integrated to 0.1.

X_t	$\frac{\partial X_t}{\partial t}$	$\frac{\partial X_t}{\partial W_{1t}}$	$\frac{\partial X_t}{\partial W_{2t}}$	$\frac{\partial X_t}{\partial W_{3t}}$	$\frac{\partial X_t}{\partial W_{4t}}$
P_t	$f(10 + 12V_{2t}) - \frac{1}{2}F_t^2$ $+\frac{1}{2} \left[13 - 13(1 + 33V_{3t}) + \frac{1}{2} 14 - 14(1 + 44V_{4t}) \right] F_t \log P_t$	$F_t P_t$	0	$13F_t P_t$	$14F_t P_t$
V_{2t}	$22V_{2t}$	0	1	0	0
V_{3t}	$33V_{3t} - \frac{1}{2} 33(1 + 33V_{3t})$	0	0	$1 + 33V_{3t}$	0
V_{4t}	$44V_{4t} - \frac{1}{2} 44(1 + 44V_{4t})$	0	0	0	$1 + 44V_{4t}$

TABLE X III: Derivatives for Log Linear model with feedback. Here $F_t = e^{10 + 13V_{3t} + 14V_{4t}}$ and $\frac{\partial X_t}{\partial W_{1t}} = 1 - \frac{2}{13} - \frac{2}{14}$.

We examined quantities $\overline{\ln P_t}$, $\overline{V_{2t}}$, $\overline{V_{3t}}$, and $\text{var}(V_{3t})$ some of which have exact solutions

$$\overline{V_{2t}} = V_{20} e^{22t} \quad (43)$$

$$\overline{V_{3t}} = V_{30} e^{33t} \quad (44)$$

$$\begin{aligned} \text{var}(V_{3t}) = & (V_{30})^2 (e^{(2_{33} + \frac{2}{33})t} - e^{2_{33}t}) + \frac{2_{33}V_{30}}{33 + \frac{2}{33}} (e^{(2_{33} + \frac{2}{33})t} - e^{33t}) \\ & + \frac{1}{2_{33} + \frac{2}{33}} (e^{(2_{33} + \frac{2}{33})t} - 1): \end{aligned} \quad (45)$$

We obtained $\overline{\ln P_t}$ numerically by solving the ordinary differential equation

$$\frac{d\overline{\ln P_t}}{dt} = -10 + 12V_{20}e^{22t} - \frac{e^{2_{10}}}{2} \frac{\overline{e^{2_{13}V_{3t}}}}{e^{2_{14}V_{4t}}} \quad (46)$$

using a variable-stepsize Runge-Kutta scheme [15]. The averages $\overline{e^{2_{1i}V_{it}}}$ for $i = 3, 4$ were obtained from the moments $\overline{(V_{it})^n}$ using $\overline{e^{xV_{it}}} = \sum_{n=0}^{\infty} \frac{x^n}{n!} \overline{(V_{it})^n}$ (numerically truncated after $n = 20$) and iteration using

$$\begin{aligned} \overline{V_{it}} &= V_{i0} e^{iit} \quad (47) \\ \overline{(V_{it})^2} &= (V_{i0})^2 e^{(2_{ii} + \frac{2}{ii})t} + \frac{2_{ii}V_{i0}}{ii + \frac{2}{ii}} (e^{(2_{ii} + \frac{2}{ii})t} - e^{iit}) + \frac{1}{2_{ii} + \frac{2}{ii}} (e^{(2_{ii} + \frac{2}{ii})t} - 1) \quad (48) \\ \overline{(V_{it})^n} &= (V_{i0})^n e^{(n_{ii} + \frac{n(n-1)}{2} \frac{2}{ii})t} + n(n-1) \frac{2_{ii}}{ii} \int_0^t dt^0 \overline{(V_{it^0})^{n-1}} e^{(n_{ii} + \frac{n(n-1)}{2} \frac{2}{ii})(t-t^0)} \\ &+ \frac{n(n-1)}{2} \int_0^t dt^0 \overline{(V_{it^0})^{n-2}} e^{(n_{ii} + \frac{n(n-1)}{2} \frac{2}{ii})(t-t^0)}; \quad \text{for } n = 3, 4, \dots \quad (49) \end{aligned}$$

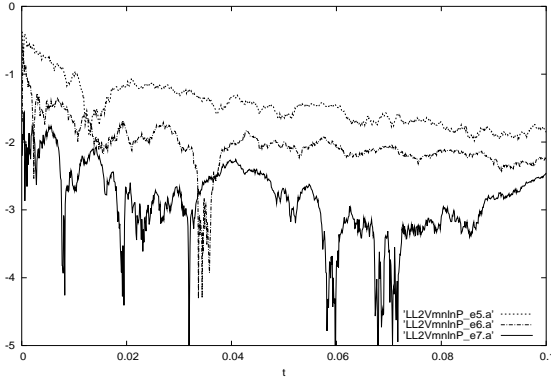
which are also readily obtained using an ODE code.

The parameters were set as $10 = :0279$, $12 = :7281$, $22 = 5.9997$, $33 = :1227$, $44 = 8.2119$, $10 = :0486$, $13 = :0695$, $14 = :3130$, $33 = :3672$, $44 = :3655$, $13 = :1077$, $14 = :0564$, with initial conditions $P_0 = 1$, $V_{20} = :1$, $V_{30} = :05$, $V_{40} = :2$.

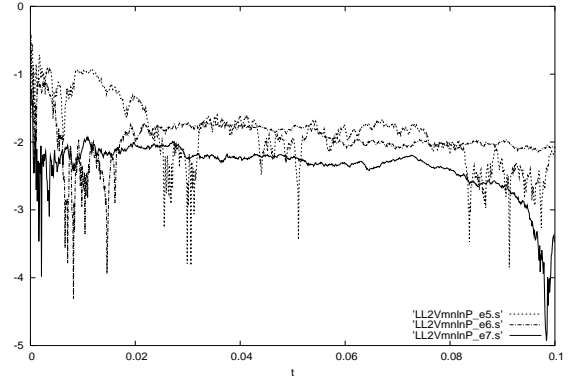
In Fig. 13 we plot the log base ten relative accuracy of $\overline{\ln P_t}$ and $\overline{V_{2t}}$ against time for ANISE ((a) and (c), respectively) and SDE9 ((b) and (d), respectively). The dashed curve represents an average over 10^5 trajectories, while the dot-dashed and solid curves represent calculations with 10^6 and 10^7 trajectories, respectively. In all cases convergence is good except for $\overline{\ln P_t}$ in the vicinity of zero where the exact solution vanishes and the relative accuracy becomes poorly defined.

Figure 14 plots the error in $\overline{V_{3t}}$ and $\text{var}(V_{3t})$ for ANISE and SDE9. Good convergence is observed in all cases. Errors in the mean are greater than those in the variance.

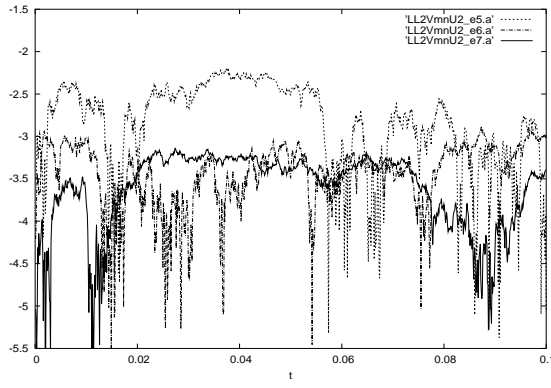
The cpu times for various numbers of trajectories are given in Table XIV. ANISE takes 7.5 s to compute 1000 trajectories. Once again ANISE is about twice as fast as SDE9.



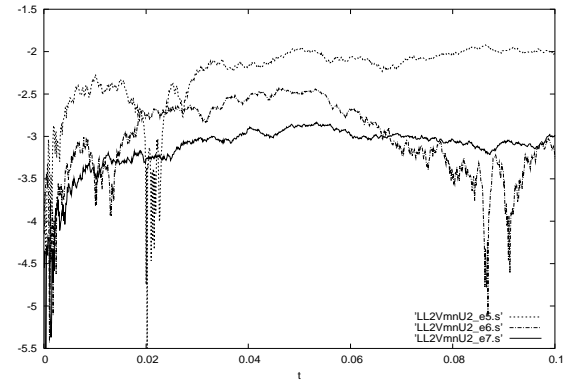
(a) $\overline{\ln P_t}$ vs. t for ANISE



(b) $\overline{\ln P_t}$ vs. t for SDE9



(c) $\overline{V_{2t}}$ vs. t for ANISE



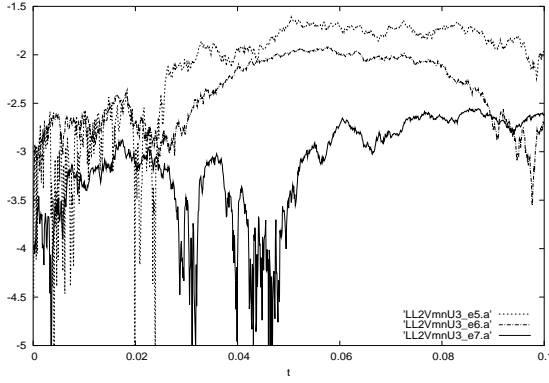
(d) $\overline{V_{2t}}$ vs. t for SDE9

FIG .13: Means of $\ln P_t$ and V_{2t} for Log Linear model with feedback

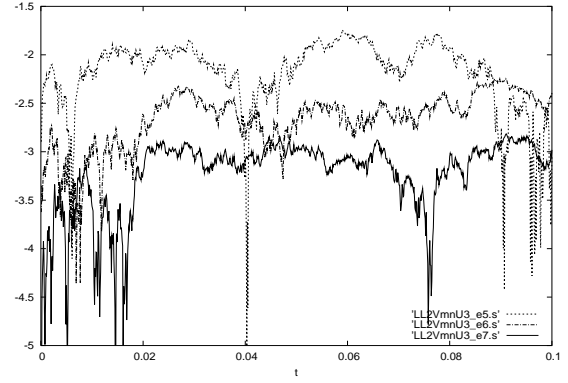
III. ACCURACY FOR INDIVIDUAL TRAJECTORIES

Here we again request a relative accuracy of 10^{-12} and determine what accuracy is in fact obtained on average for individual trajectories. While it is unlikely that results of this high precision would be required in actual financial applications, it is worth exploring this issue for a few problems where exact solutions of the SODEs are known. We find that the calculations are not very sensitive to the requested tolerance, and accuracies of 10^{-12} are sometimes achieved even when the requested tolerance is only 10^{-6} . The calculations are also insensitive to the stepsize.

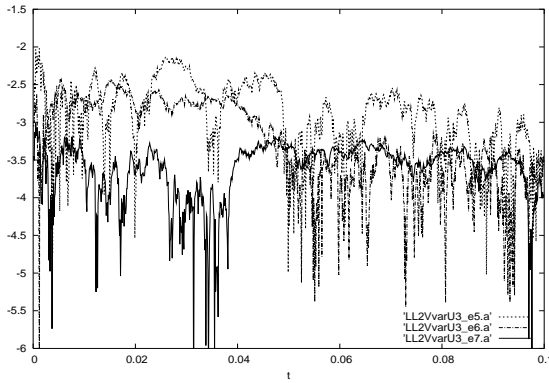
For each realization of the observable we thus calculate an exact solution X_t and an



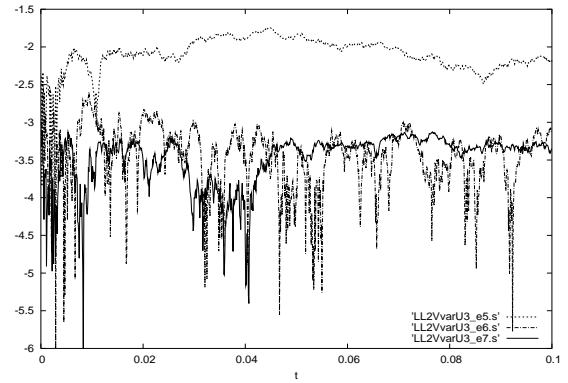
(a) $\overline{V_{3t}}$ vs. t for AN ISE



(b) $\overline{V_{3t}}$ vs. t for SDE 9



(c) $\text{var}(V_{3t})$ vs. t for AN ISE



(d) $\text{var}(V_{3t})$ vs. t for SDE 9

FIG . 14: Error in mean and variance of V_{3t} for Log Linear model with feedback

approximate solution X_t^{approx} from which we compute the log base ten relative error

$$\log_{10} \left[\frac{|X_t - X_t^{\text{approx}}|}{\max(|X_t|, |X_t^{\text{approx}}|)} \right] \quad (50)$$

We plot the average of this quantity against time t for each model. The exact solutions involve some difficult integrals which are also computed using the numerical method, so our tests are essentially self-consistency checks.

For both models we have requested large time steps and integrated to very long times in order to make the calculation somewhat challenging. The errors shown are computed as time averages over short intervals since there are high frequency fluctuations in the data which make identification of the line types in the figures difficult.

# Trajectories	ANISE CPU Time	SDE9 CPU Time	CPU Time Ratio SDE9/ANISE
10^3	0.74E+ 01	0.15E+ 02	2.04
10^4	0.75E+ 02	0.15E+ 03	2.06
10^5	0.74E+ 03	0.16E+ 04	2.08
10^6	0.75E+ 04	0.15E+ 05	2.08
10^7	0.75E+ 05	0.15E+ 06	2.08

TABLE XIV : CPU times for Log Linear model with feedback in seconds.

A . Vasicek interest rate model

The SODE for this model is

$$dV_t = c(V_t)dt + \sigma dW_t; \quad (51)$$

which has the solution

$$V_t = V_0 e^{-\alpha t} + (1 - e^{-\alpha t}) + e^{\alpha t} \int_0^t e^{-\alpha s} \sigma dW_s; \quad (52)$$

The derivatives needed by the numerical methods are given in Table XV .

M odel	$\frac{\partial V_t}{\partial t}$	$\frac{\partial V_t}{\partial W_t}$
Vasicek	$c(V_t)$	
CEV	$(V_t)^{\frac{1}{2}} V_t$	V_t

TABLE XV : equation array for Vasicek and CEV Models

We set the parameters to $c = .05$, $\sigma = .09$, $\alpha = .03$, and $V_0 = .08$. We set the time step to $dt = .24$ and integrated to 12000. This is of course a very long dynamics. We plot the average relative error in Fig. 15 (a) for ANISE (solid curve) and SDE9 (dot-dashed curve). Both ANISE and SDE9 return results consistent with the requested tolerance. SDE9 returns a greater relative tolerance than that requested.

The cpu times are compared in Table XVI. Here we see that SDE9 also runs somewhat faster than ANISE for this problem .

M odel	A N ISE	S D E 9	R atio S D E 9/A N ISE
V asicek	.79E+ 05	.57E+ 05	0.72
C EV	.37E+ 05	.65E+ 05	1.75

TABLE XVI: CPU times for $\text{tol} = 10^{-12}$ and 1 million trajectories.

B . M ean-reverting C EV m odel

Here the SODE is of the form [3]

$$dV_t = (\mu - \sigma^2 V_t)dt + \sigma V_t dW_t \quad (53)$$

which has the exact solution

$$V_t = \exp\left(\left(\mu - \frac{\sigma^2}{2}\right)t + \sigma W_t\right) \left[V_0 + \int_0^t ds \exp\left(-\left(\mu - \frac{\sigma^2}{2}\right)s - \sigma W_s\right) g\right] \quad (54)$$

The derivatives needed by the numerical methods are given in Table XV .

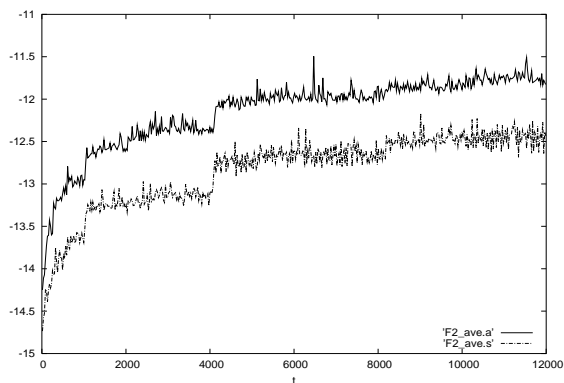
The parameters were chosen as $\mu = .05$, $\sigma = .09$, $\gamma = .1$, and $V_0 = .08$. We set the time step to $dt = .5$ and integrated to 10000. The average relative error is plotted in Fig. 15 (b) for ANISE (solid curve) and SDE9 (dot-dashed curve). Both ANISE and SDE9 return results consistent with the requested tolerance. Once again SDE9 returns a better relative tolerance than that requested.

Table XVI contains the cpu times for the two methods. SDE9 takes 75 % longer than ANISE .

IV . C O N C L U S I O N S

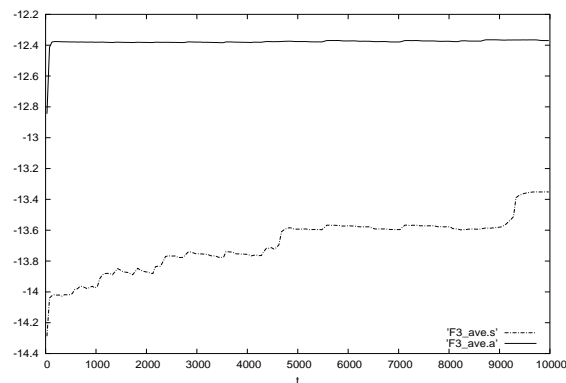
Good convergence is obtainable using both ANISE and SDE9 for all the problems considered. In most cases ANISE runs roughly twice as fast. For the Vasicek model in section III SDE9 performed 40 % faster than ANISE . ANISE performed several hundreds of times faster than SDE9 for the A ne model in section II.

In addition to our study of convergence, we examined the accuracy of individual trajectories for a given requested relative accuracy. We found that both methods returned trajectories with relative accuracies consistent with the accuracy requested, even for very long integration times.



(a) ANISE (solid) and SDE9 (dot-dashed)

for Vasicek.



(b) ANISE (solid) and SDE9 (dot-dashed)

for CEV.

FIG. 15: Average error in volatility V_t for individual trajectories.

Both algorithms appear to be sufficiently accurate for the models considered. ANISE performed better overall. The two methods appear capable of handling larger systems of equations with more Wiener processes, and could therefore prove to be valuable computational tools for further research in finance.

ACKNOWLEDGMENTS

JW. acknowledges the support of the Natural Sciences and Engineering Research Council of Canada.

-
- [1] Pearson N D and Sun T.-S. 1994 Exploiting the conditional density in estimating the term structure: an application to the Cox, Ingersoll, and Ross model *J. Finance* 49, 1279-1304
 - [2] Cox J.C., Ingersoll J.E. and Ross S.A. 1985 An intertemporal general equilibrium model of asset prices *Econometrica* 53, 363-384
 - [3] Cox J.C., Ingersoll J.E. and Ross S.A. 1985 A theory of the term structure of interest rates *Econometrica* 53, 385-407
 - [4] Davis, M.H.A. 2004 Complete-market models of stochastic volatility, *Proc. Roy. Soc. Lond. A* 460, 11-26

- [5] Hull J. and White A .1987 The pricing of options with stochastic volatilities J. Finance 42, 281-300
- [6] Hull J. and White A .1988 An analysis of the bias in option pricing caused by a stochastic volatility Adv. Futures Opt. Res. 3, 29-61
- [7] Scott, L .1987 Option pricing when the variance changes randomly: theory, estimation and an application J. Financial and Quantitative Analysis 22, 419-438
- [8] Nelson D B .1990 ARCH models as diffusion approximations J. Econometrics 45, 7-38
- [9] Anderson T G .and Bollerslev T .1998 Answering the Sceptics: yes, standard volatility models do provide accurate forecasts International Economic Review 39, 885-905
- [10] Hobson D G .and Rogers L C G .1998 Complete models with stochastic volatility Mathematical Finance 8, 27-48
- [11] Du e D .K an R .1996 A yield-factor model of interest rates Mathematical Finance 6, 379-406
- [12] Chernov M ., Gallant A R ., Ghysels E .and Tauchen G .2003 Alternative models for stock price dynamics J. Econometrics 116, 225-257
- [13] Engle R F .1982 Autoregressive conditional heteroscedasticity with estimates of the variance of United Kingdom inflation Econometrica 50, 987-1007
- [14] Kloeden P E . and Platen E . 1992 Numerical Solution of Stochastic Differential Equations (Berlin: Springer)
- [15] Hairer E ., Norsett S P .and Wanner G .1993 Solving Ordinary Differential Equations (Berlin: Springer-Verlag)
- [16] See <http://www.math.uni-frankfurt.de/~numerik/mplestoch/>
- [17] Gaines J G .1997 Variable step size control in the numerical solution of stochastic differential equations SIAM J. Appl. Math. 57, 1455-1484
- [18] Lamba H .2003 An adaptive time stepping algorithm for stochastic differential equations J. Comput. Appl. Math. 161, 417-430
- [19] Wilkie J .2004 Numerical methods for stochastic differential equations Phys. Rev. E 70, 017701
- [20] Wilkie J. and Cetinbas M . 2005 Variable-stepsize Runge-Kutta methods for stochastic Schrodinger equations Phys. Lett. A 337, 166-182
- [21] ANISE ^C (available as a free trial), from Innovative Stochastic Algorithms
- [22] Vasioek, O .1977 An equilibrium characterization of the term structure J. Financial Economics 5, 177-188